

## Internal Excitation and Ionization Accompanying $K$ Capture

Takeshi Mukoyama, Yasuhito Isozumi, Tetsuo Kitahara, and Sakae Shimizu

*Institute for Chemical Research and Radioisotope Research Center, Kyoto University, Kyoto, Japan*

(Received 11 June 1973)

The internal excitation and ionization probabilities during  $K$ -electron capture have been treated relativistically by the use of hydrogenic wave functions. Relativistic and nonrelativistic calculations for the double  $K$ -hole production probability, the total internal ionization probability, and the energy spectrum of the ejected electrons are presented. The present calculations show that the relativistic effects cause a substantial reduction in the probabilities. The calculated probabilities of the double  $K$ -hole production and the total internal ionization have been compared with the experimental values, and there has been fairly good agreement between the calculated and the recently measured values. The spectral shape of the ejected electrons calculated from the present relativistic theory is similar to that obtained from the previous nonrelativistic and relativistic theories. The theoretical curves are in good agreement with the experimental results in the high-energy region. The discrepancies between the theory and the various experiments are discussed and further work is suggested.

### I. INTRODUCTION

In the usual theory of nuclear decay a radioactive nucleus is treated as bare and contributions from the atomic electrons are neglected. However, there are some nuclear-decay processes in which the atomic variables should be included in the description of a radioactive system. When a nucleus undergoes nuclear disintegration by emission or absorption of an electron, the remaining electrons in the atom experience a sudden change in nuclear charge. This may cause electronic excitation to an unoccupied bound state (internal excitation) or ionization to the continuum (internal ionization). For the case of negatron emission, theoretical estimates of the internal ionization probability were first made by Feinberg<sup>1</sup> and Migdal<sup>2</sup> in 1941. Since this early work, many experimental and theoretical studies have been performed for  $\beta^-$  decay.<sup>3</sup>

On the other hand, the role of the electron *corollège* in electron capture was first studied by Benoist-Gueutal<sup>4</sup> in 1950. She found that the probability for  $L$ -electron capture of  ${}^7\text{Be}$  is double that given by the ordinary theory. The first theoretical study of the process where the atom is excited or ionized internally during electron capture was made by Primakoff and Porter<sup>5</sup> in 1953. Using nonrelativistic variational wave functions for the two  $K$  electrons in the parent atom, they obtained expressions for the double  $K$ -hole production probability and for the total  $K$ -shell internal ionization probability per  $K$  capture, as well as for the momentum distribution of the ejected  $K$  electrons.

Intemann and Pollock<sup>6</sup> also calculated nonrelativistically the momentum distribution of the ejected  $K$  electrons. They treated the electron-electron interaction as a perturbation of the nuclear Coulomb interaction of the system. The predicted spectrum is identical with that obtained by the Primakoff-Porter (PP) theory. As an extension of his earlier work,<sup>6</sup> Intemann<sup>7,8</sup> treated the phenomenon relativistically. He obtained the results that relativistic effects have only slight influence on the shape of the energy spectrum of the ejected  $K$  electrons, but reduce the total  $K$ -ejection probability approximately by a factor of 2.

In analogy with the case of  $\beta^-$  decay, Stephas<sup>9</sup> obtained analytical expressions for the  $K$ -ionization probability and the spectral distribution of the ejected  $K$  electrons during  $K$  capture, using the atomic matrix element of Stephas and Crasemann<sup>10,11</sup> with relativistic hydrogenic wave functions. However, the probability calculated from their corrected matrix element diverges in the small-momentum limit of the ejected  $K$  electrons, because of an approximation made in the evaluation of the contour integral.<sup>12</sup>

In the present work, we provide a more accurate relativistic treatment of the internal excitation and ionization of  $K$ -shell electrons accompanying  $K$  capture, using an exact matrix element obtained from relativistic hydrogenic wave functions without any approximation.

In the present work, we provide a more accurate relativistic treatment of the internal excitation and ionization of  $K$ -shell electrons accompanying  $K$  capture, using an exact matrix element obtained from relativistic hydrogenic wave functions without any approximation.

### II. GENERAL FORMALISM

In a complete description of electron capture, the probability that a  $K$  electron, initially in the state  $\psi_i(Z, K)$ , makes a transition to a final state  $\psi_f(Z', W)$  during the capture of another  $K$  electron

$\psi'(Z, K)$  is<sup>13</sup>

$$w dW = 2\pi |\langle \psi_f(Z', W) \psi_\nu \psi_f(N) | H_\beta | \psi_i(N) \psi'(Z, K) \psi_i(Z, K) \rangle|^2 \rho(\nu, e), \quad (1)$$

where  $\psi_i(N)$  and  $\psi_f(N)$  are the initial and final nuclear wave functions,  $\psi_\nu$  is the neutrino wave function,  $H_\beta$  is the weak-interaction Hamiltonian, and  $\rho(\nu, e)$  is the density of final states. The units are such that  $\hbar = m = c = 1$ .

This equation can be rewritten in the form of a product of atomic and nuclear parts as follows:

$$w dW = 2\pi |\langle \psi_i \psi_f(N) | H_\beta | \psi_i(N) \psi'(Z, K) \rangle|^2 \times |\langle \psi_f(Z', W) | \psi_i(Z, K) \rangle|^2 \rho(\nu, e). \quad (2)$$

In this expression, the first factor, which is the nuclear part, represents the matrix element of ordinary  $K$  capture, and the second factor, the atomic matrix element, is the overlap of electron wave functions between initial and final states, usually neglected in the theory of electron capture.

The energy balance of electron-capture decay corresponding to Eq. (2) is given by

$$M_i + 2(1 - B_K) = M_f + q_\nu + W, \quad (3)$$

where  $M_i$  and  $M_f$  are the nuclear masses (in units of energy) in the initial and final states,  $B_K$  is the  $K$ -shell binding energy of the daughter atom,  $q_\nu$  is the energy carried off by the neutrino, and  $W$  is the total energy (including the rest mass) of the uncaptured  $K$  electron in the final state.

In ordinary electron capture, all the remaining electrons are assumed to retain their original quantum numbers in the daughter atom, and the atomic-wave-function overlap, nearly unity in this case, is neglected. The probability for  $K$ -electron capture is given by<sup>9</sup>

$$w_K = \pi^{-1} G^2 g_K^2(R) |M_N|^2 S(W_0) W_0^2, \quad (4)$$

where  $G$  denotes the coupling constant of the weak interaction,  $g_K^2(R)$  is the density of the  $K$  electron at the nuclear surface,  $M_N$  is the energy-independent part of the nuclear matrix element, and  $S(W_0)$  is the energy-dependent shape factor. The transition energy  $W_0$  is

$$W_0 = M_i - M_f - B_K + 1. \quad (5)$$

In normal approximation, the shape factor for the nuclear transition  $I_i \rightarrow I_f$  is expressed as<sup>14</sup>

$$S(W_0) = (W_0 R)^{2(\Delta I - 1)} / [(2\Delta I - 1)!!]^2, \quad (6)$$

where  $R$  denotes the nuclear radius,  $\Delta I = |I_i - I_f|$  for  $I_i \neq I_f$ , and  $\Delta I = 1$  for  $I_i = I_f$ .

Because of conservation of orbital angular momentum, the remaining  $K$ -shell (1s) electron can make a transition only to an unoccupied bound state represented by  $ns$ . Then the energy avail-

able to the neutrino is obtained from Eq. (3) as

$$W_n = W_0 - B_K + B_n, \quad (7)$$

where  $B_n$  is the binding energy of the electron in the  $ns$  state of the daughter atom. The transition probability of the other  $K$ -shell electron to the  $ns$  state during  $K$  capture is

$$w_{Kn} = \pi^{-1} G^2 g_K^2(R) |M_N|^2 S(W_n) W_n^2 |M_{Kn}|^2, \quad (8)$$

where  $M_{Kn} = \langle \psi_f(Z', n) | \psi_i(Z, K) \rangle$  is the atomic-wave-function overlap of the 1s state of the parent atom with the  $ns$  state of the daughter. From Eqs. (4) and (8), the probability per  $K$  capture that the remaining  $K$  electron in the parent atom undergoes a transition to the  $ns$  state of the daughter is

$$P_{Kn} = w_{Kn} / w_K = (W_n / W_0)^2 [S(W_n) / S(W_0)] |M_{Kn}|^2. \quad (9)$$

Let  $n'$  be the highest occupied state of the parent atom; then the internal excitation probability per  $K$  capture is

$$P_{ex} = \sum_{n=n'+1}^{\infty} P_{Kn}. \quad (10)$$

On the other hand, when one  $K$  electron is captured, the internal ionization probability for the other  $K$  electron to be ejected with total energy  $W$  is<sup>9</sup>

$$w(W) dW = (G^2 / 2\pi^3) g_K^2(R) |M_N|^2 |M_A|^2 (W_K - W)^2 \times S(W_K - W) pW dW, \quad (11)$$

where  $W_K$  denotes

$$W_K = W_0 + 1 - B_K. \quad (12)$$

The internal ionization probability per  $K$  capture is found from Eqs. (4) and (11) as

$$P(W) dW = \frac{1}{2\pi^2} |M_A|^2 \frac{S(W_K - W)}{S(W_0)} \frac{(W_K - W)^2}{W_0^2} pW dW. \quad (13)$$

The total ionization probability per  $K$  capture is given by

$$P_{ej} = \int_1^{W_K} P(W) dW. \quad (14)$$

The completeness theorem leads to the relation

$$1 = \sum_{n=1}^{\infty} P_{Kn} + P_{ej}. \quad (15)$$

Therefore, the probability per  $K$  capture of producing double holes in the  $K$  shell of the daughter

atom is

$$P(2) = P_{\text{ex}} + P_{\text{ej}} \\ = 1 - \sum_{n=1}^{n'} P_{Kn}. \quad (16)$$

In the theory of Primakoff and Porter<sup>5</sup> and Levinger,<sup>15</sup>  $P(2)$  is expressed in terms of  $P_{KK}$ , the probability that the uncaptured  $K$  electron still remains in the  $K$  shell of the daughter, as follows:

$$P(2) = \xi(1 - P_{KK}), \quad (17)$$

where  $\xi$  accounts for the occupied states of the daughter atom excluded by the Pauli principle.

### III. ATOMIC MATRIX ELEMENTS

#### A. Atomic Matrix Element for $K$ -Shell Internal Ionization

The atomic matrix element for  $K$ -shell internal ionization is given as wave-function overlap:

$$M_A = \langle \psi_f(Z', W) | \psi_i(Z, K) \rangle. \quad (18)$$

Here  $\psi_i(Z, K)$  is the wave function of a  $K$ -shell

electron of the parent atom with the atomic number  $Z$ , and  $\psi_f(Z', W)$  is the wave function for a continuum electron with total energy  $W$  in the Coulomb field of the daughter nucleus of the charge  $Z'$ .

The  $K$ -shell Coulomb wave function is given by<sup>16</sup>

$$\psi_i(Z, K) = \begin{pmatrix} g_{-1}(\zeta, r) \chi_{-1}^{\mu}(\hat{r}) \\ if_{-1}(\zeta, r) \chi_1^{\mu}(\hat{r}) \end{pmatrix}, \quad (19)$$

with  $\mu = \pm \frac{1}{2}$ . The radial functions  $g_{-1}(\zeta, r)$  and  $f_{-1}(\zeta, r)$  are

$$g_{-1}(\zeta, r) = N(1 + \gamma)^{1/2} r^{\gamma-1} e^{-\zeta r}, \quad (20a)$$

$$f_{-1}(\zeta, r) = -N(1 - \gamma)^{1/2} r^{\gamma-1} e^{-\zeta r}, \quad (20b)$$

where  $\zeta = \alpha Z$ ,  $\gamma^2 = 1 - \zeta^2$ ,  $N = \{(2\zeta)^{2\gamma+1} / [2\Gamma(2\gamma+1)]\}^{1/2}$ ,  $\alpha$  is the fine-structure constant, and  $\chi_k^{\mu}(\hat{r})$  is the spin-angular function.

The continuum wave function in the Coulomb field is<sup>17</sup>

$$\psi_f(Z', W) = \begin{pmatrix} g_{\kappa}(\zeta', r) \chi_{\kappa}^{\mu}(\hat{r}) \\ if_{\kappa}(\zeta', r) \chi_{-\kappa}^{\mu}(\hat{r}) \end{pmatrix}. \quad (21)$$

The radial functions in this expression are

$$f_{\kappa}(\zeta', r) = i \left( \frac{W-1}{2W} \right)^{1/2} \frac{2\pi^{1/2} (2pr)^{\gamma'-1} e^{\pi y/2} |\Gamma(\gamma'+iy)|}{\Gamma(2\gamma'+1)} \{ e^{-ipr+i\eta} (\gamma'+iy) F(\gamma'+1+iy, 2\gamma'+1; 2ipr) - \text{c.c.} \}, \quad (22a)$$

$$g_{\kappa}(\zeta', r) = \left( \frac{W+1}{2W} \right)^{1/2} \frac{2\pi^{1/2} (2pr)^{\gamma'-1} e^{\pi y/2} |\Gamma(\gamma'+iy)|}{\Gamma(2\gamma'+1)} \{ e^{-ipr+i\eta} (\gamma'+iy) F(\gamma'+1+iy, 2\gamma'+1; 2ipr) + \text{c.c.} \}, \quad (22b)$$

where  $W^2 = p^2 + 1$ ,  $\zeta' = \alpha Z'$ ,  $\gamma'^2 = \kappa^2 - \zeta'^2$ ,  $y = \zeta'W/p$ ,  $F(\alpha, \beta; x)$  is the confluent hypergeometric function, and c.c. denotes complex conjugate. The factor  $\eta$  is given by

$$e^{2i\eta} = -(\kappa - iy/W) / (\gamma' + iy).$$

Using the above representations, the overlap integral can be written as follows:

$$\langle \psi_f(Z', W) | \psi_i(Z, K) \rangle = \int_0^{\infty} r^2 dr [g_{-1}(\zeta', r)g_{-1}(\zeta, r) + f_{-1}(\zeta', r)f_{-1}(\zeta, r)]. \quad (23)$$

A technique similar to that used by Jaeger and Hulme<sup>18</sup> in the calculation of internal conversion is applied to the radial integrals in Eq. (23). Writing

$$u = \frac{2p}{p - i\zeta'}, \quad v = \frac{2\zeta}{p - i\zeta}, \quad w = \frac{1}{p - i\zeta},$$

we find the overlap integral reduces to

$$M_A = (-i)^{\gamma'+\gamma+1} 2\pi^{1/2} e^{\pi y/2+i\eta} N u^{\gamma'-1} v^{\gamma-1} w^3 \frac{\Gamma(\gamma'+\gamma+1)}{\Gamma(2\gamma'+1)} |\Gamma(\gamma'+iy)| \\ \times [( \gamma'+iy) A F(\gamma+\gamma'+1, \gamma'+1+iy; 2\gamma'+1; u) + (1 - iy/W) A^* F(\gamma+\gamma'+1, \gamma'+iy; 2\gamma'+1; u)], \quad (24)$$

where  $F(\alpha, \beta; \gamma; x)$  is the hypergeometric function, and

$$A = \left( \frac{W+1}{2W} \right)^{1/2} (1+\gamma)^{1/2} - i \left( \frac{W-1}{2W} \right)^{1/2} (1-\gamma)^{1/2}.$$

The nonrelativistic limit of this expression is obtained by letting  $W = \gamma = \gamma' = 1$ . Then we can write the square of the matrix element  $|M_{\text{nr}}|^2$  in the following form:

$$|M_{\text{nr}}|^2 = \frac{2^7 \pi^2 \zeta^5 \zeta'}{Z^2 (p^2 + \zeta^2)^4} \frac{e^{-4y \tan^{-1}(p/\zeta)}}{1 - e^{-2\pi y}}. \quad (25)$$

This result agrees with the nonrelativistic expression obtained by Stephas and Crasemann,<sup>11</sup> and that of Primakoff and Porter.<sup>5</sup>

In the small-momentum limit, Eq. (24) becomes

$$\lim_{p \rightarrow 0} M_A \sim 2^{\gamma+\gamma'-1/2} \pi \xi^{-(\gamma+2)} p^{-1/2} \xi^{\gamma-1/2} N \frac{\Gamma(\gamma+\gamma'+1)}{\Gamma(2\gamma'+1)} \\ \times \{(\gamma' - \gamma)(1 + \gamma)^{1/2} F(\gamma + \gamma', 2\gamma' + 1; -2\xi'/\xi) \\ + [(1 + \gamma)^{1/2}(\gamma + 1 - 2\xi'/\xi) + (1 - \gamma)^{1/2}\xi'] F(\gamma + \gamma' + 1, 2\gamma' + 1; -2\xi'/\xi)\}. \quad (26)$$

Equation (26) implies that the ionization probability  $P(W) dW$ , proportional to  $|M_A|^2 p W dW$ , converges to a finite value as  $p \rightarrow 0$ . The nonrelativistic limit of this expression, obtained by letting  $W = \gamma = \gamma' = 1$ , reduces to the same form as Eq. (25):

$$\lim_{p \rightarrow 0} |M_{nr}|^2 \sim \frac{2^7 \pi^2 \xi'}{Z^2 \xi^3 p} e^{-4\xi'/\xi}. \quad (27)$$

#### B. Atomic Matrix Element for $K$ -Shell Internal Excitation

The atomic matrix element of the uncaptured  $K$ -shell electron in the parent atom making a transition to the  $ns$  state of the daughter atom is

$$M_{Kn} = \langle \psi_f(Z', n) | \psi_i(Z, K) \rangle, \quad (28)$$

where  $\psi_f(Z', n)$  is the wave function of the electron in the  $ns$  state of the daughter atom.

The wave function of the daughter atom is given by<sup>19</sup>

$$\psi_f(Z', n) = \begin{pmatrix} g_{-1}^{(n)}(\mathbf{r}) \chi_{-1}^{\mu}(\hat{\mathbf{r}}) \\ i f_{-1}^{(n)}(\mathbf{r}) \chi_1^{\mu}(\hat{\mathbf{r}}) \end{pmatrix}. \quad (29)$$

The radial functions  $g_{-1}^{(n)}(\mathbf{r})$  and  $f_{-1}^{(n)}(\mathbf{r})$  are

$$g_{-1}^{(n)}(\mathbf{r}) = \frac{(2\lambda^5)^{1/2}}{\Gamma(2\gamma'+1)} \left[ \frac{\Gamma(2\gamma'+n)(1+W)}{(n-1)! \xi'(\xi'+\lambda)} \right]^{1/2} (2\lambda r)^{\gamma'-1} e^{-\lambda r} \\ \times [-(n-1)F(-n+2, 2\gamma'+1; 2\lambda r) + (1+\xi'/\lambda)F(-n+1, 2\gamma'+1; 2\lambda r)], \quad (30a)$$

$$f_{-1}^{(n)}(\mathbf{r}) = \frac{(2\lambda^5)^{1/2}}{\Gamma(2\gamma'+1)} \left[ \frac{\Gamma(2\gamma'+n)(1-W)}{(n-1)! \xi'(\xi'+\lambda)} \right]^{1/2} (2\lambda r)^{\gamma'-1} e^{-\lambda r} \\ \times [(n-1)F(-n+2, 2\gamma'+1; 2\lambda r) + (1+\xi'/\lambda)F(-n+1, 2\gamma'+1; 2\lambda r)], \quad (30b)$$

where  $\xi' = \alpha Z'$ ,  $\gamma'^2 = 1 - \xi'^2$ ,  $W = (n + \gamma' - 1) / [(n + \gamma' - 1)^2 + \xi'^2]^{1/2}$ , and  $\lambda^2 = 1 - W^2$ .

With the aid of the above representations for the initial and final electron wave functions, we can with some algebra obtain an analytic expression for the matrix element:

$$M_{Kn} = \frac{\Gamma(\gamma+\gamma'+1)}{\Gamma(2\gamma'+1)} \frac{2^{\gamma+\gamma'-1/2} \xi^{\gamma+1/2} \lambda^{\gamma'+3/2}}{(\xi+\lambda)^{\gamma+\gamma'+1}} \left[ \frac{1}{(n-1)! \xi'(\xi'+\lambda)} \frac{\Gamma(2\gamma'+n)}{\Gamma(2\gamma'+1)} \right]^{1/2} \\ \times \{ (n-1) [(1-\gamma)^{1/2}(1-W)^{1/2} - (1+\gamma)^{1/2}(1+W)^{1/2}] F(\gamma+\gamma'+1, -n+2; 2\gamma'+1; 2\lambda/(\lambda+\xi)) \\ + (1+\xi'/\lambda) [(1+\gamma)^{1/2}(1+W)^{1/2} + (1-\gamma)^{1/2}(1-W)^{1/2}] F(\gamma+\gamma'+1, -n+1; 2\gamma'+1; 2\lambda/(\lambda+\xi)) \}. \quad (31)$$

Especially in the case where the  $K$  electron remains in the  $K$  shell of the daughter atom, Eq. (31) attains the simpler form

$$M_{KK} = \frac{\Gamma(\gamma+\gamma'+1)}{[\Gamma(2\gamma'+1)\Gamma(2\gamma'+1)]^{1/2}} \frac{2^{\gamma+\gamma'} \xi^{\gamma+1/2} \lambda^{\gamma'+1/2}}{(\lambda+\xi)^{\gamma+\gamma'+1}} [(1+\gamma)^{1/2}(1+\gamma')^{1/2} + (1-\gamma)^{1/2}(1-\gamma')^{1/2}]. \quad (32)$$

#### IV. ESTIMATION OF SCREENING CONSTANTS AND $\xi$

To take account of the effects of Coulomb interaction and spacial correlation of the electrons, the charge  $Z$  in the hydrogenic wave functions is replaced by an appropriate effective charge  $Z_{\text{eff}}$

$= Z - \sigma$ . The choice of the screening constant  $\sigma$  is of particular importance and significance. Primakoff and Porter<sup>5</sup> and Stephas<sup>9</sup> have used the constant value 0.5 for  $K$  electrons of all elements, which is deduced from the Hylleraas nonrelativistic variational wave function. However,  $\sigma$  should be a function of the atomic number.

In the definition by Hartree,<sup>20</sup>  $\sigma$  is determined as a function of  $Z$  from the ratio of the mean hydrogenic radius  $\bar{r}_H$  to the mean radius  $\bar{r}$  from a self-consistent-field (SCF) wave function:

$$\sigma = Z - \bar{r}_H / \bar{r}. \quad (33)$$

This choice of screening constant has been applied to the calculations of  $K$ -electron shakeoff probability accompanying  $\beta^-$  decay by Campbell, McNelles, and Law.<sup>21</sup> Using the SCF functions of Froese, they indicated that inclusion of the screening constant does not affect the shakeoff probability. The extension of Eq. (33) to the relativistic case leads to serious difficulty in that the value of  $\sigma$  for the  $K$  shell of some elements becomes negative.

A different approach to evaluate  $\sigma$  can be taken using a relativistic definition<sup>22</sup>:

$$\sigma = Z(1 - \bar{r}_Z / \bar{r}_{\text{SCF}}), \quad (34)$$

where  $\bar{r}_Z$  is the mean radius determined by the relativistic hydrogenic wave function in the Coulomb field of the atomic nucleus of charge  $Z$ , and  $\bar{r}_{\text{SCF}}$  is the mean radius determined from the relativistic SCF calculation for the same atom.

The value of the mean radius  $\bar{r}_Z$  is defined by

$$\bar{r}_Z = \int_0^\infty \psi^*(Z, n) r \psi(Z, n) d^3r. \quad (35)$$

Inserting the wave function of Eq. (29) into Eq. (35) and using an integration formula for the hypergeometric function,<sup>23</sup> the mean radius is

$$\begin{aligned} \bar{r}_Z = & \frac{\lambda}{4\Gamma(2\gamma+1)} \frac{\Gamma(2\gamma+n)}{(n-1)! \xi(\xi+\lambda)} \\ & \times [(n-1)^2 G(n-2, n-2) + (1+\xi/\lambda)^2 G(n-1, n-1) \\ & - 2W(n-1)(1+\xi/\lambda)G(n-2, n-1)], \quad (36) \end{aligned}$$

where

$$\begin{aligned} G(m, m') = & \sum_{j=0}^m \frac{(-m)_j (2\gamma+1+j)}{j!} \\ & \times F(-m', 2\gamma+2+j; 2\gamma+1; 1), \end{aligned}$$

and  $(-m)_j$  means  $(-m)(-m+1)\cdots(-m+j-1)$ . The values of  $\bar{r}_{\text{SCF}}$  are taken from the calculated results of Carlson *et al.*<sup>24</sup> In Table I the values of the screening constants for  ${}_{31}\text{Ga}$  thus estimated are shown and compared with those estimated by the Slater recipe.<sup>25</sup>

However, the use of these screening constants causes trouble in the evaluation of the double  $K$ -hole production probability using Eq. (16). In some cases, the sum of the overlap integrals of the bound-state hydrogenic wave functions becomes larger than unity. The main reasons that Eq. (15) does not hold are the following two: (1) The screened hydrogenic wave functions used here are

not orthogonal because the value of  $\sigma$  depends on the quantum number  $n$ , and (2) it is not taken into account that following electron capture the daughter atom has a hole in the  $K$  shell. To avoid these difficulties, the screening constants determined above were used only for the  $K$  shell of the parent atom, and the probability  $P(2)$  was evaluated by the use of Eq. (17). As to the daughter atom, the screening constant was estimated by Slater's recipe. According to this rule, the  $K$ -shell screening constant for the atom lacking a  $K$  electron is always zero. The same choice of screening constants was made in the evaluation of the internal ionization probability.

The factor  $\xi$  in Eq. (17) has been discussed by Primakoff and Porter,<sup>5</sup> and Levinger.<sup>15</sup> The former estimated its value to be  $\frac{2}{3}$ , while the latter took it to be  $\frac{1}{2}$ . Carlson *et al.*<sup>22</sup> have estimated the value of  $\xi$  as  $\frac{1}{2}$  for electron capture in  ${}^{131}\text{Cs}$ , using relativistic Hartree wave functions. However,  $\xi$  is not a constant but varies with atomic number  $Z$ .

Comparing Eqs. (16) and (17), this factor can be defined as

$$\xi = \frac{1 - \sum_{n=1}^{n'} (P_{Kn})_{\text{many-elec}}}{1 - (P_{KK})_{\text{many-elec}}}, \quad (37)$$

where transition probabilities  $(P_{Kn})_{\text{many-elec}}$  and  $(P_{KK})_{\text{many-elec}}$  are expressed as in Eq. (9), except that the matrix elements are calculated with SCF wave functions. We have estimated values of  $\xi$  by numerical integration using the nonrelativistic SCF wave functions of Herman and Skillman<sup>26</sup> for both parent and daughter atoms. Taking account of a hole in the  $K$  shell of the daughter atom, the calculations of the overlap integrals were made between the  $K$ -shell electron in the parent atom and the  $ns$  electron under the presence of a hole in the  $K$  shell of the daughter. The results are shown in Table II.

## V. NUMERICAL RESULTS AND COMPARISON WITH EXPERIMENTS

We have calculated the internal excitation and ionization probabilities per  $K$ -electron capture

TABLE I. Screening constant and effective nuclear charge for Ga ( $Z=31$ ).

Shell	$n$	$\sigma$	$Z_{\text{eff}}$	$\sigma_S^a$
$K$	1	0.586	30.41	0.35
$L_I$	2	3.77	27.23	4.15
$M_I$	3	10.35	20.65	11.24
$N_I$	4	20.48	10.52	26.35

<sup>a</sup> Screening constant determined from Slater's recipe.

for six nuclides,  ${}^7\text{Be}$ ,  ${}^{37}\text{Ar}$ ,  ${}^{55}\text{Fe}$ ,  ${}^{71}\text{Ge}$ ,  ${}^{131}\text{Cs}$ , and  ${}^{165}\text{Er}$ . The nuclear parameters for these nuclides are taken from the tables of Lederer, Hollander, and Perlman.<sup>37</sup> All calculations in the present work have been performed using the FACOM 230-60 computer in the Data Processing Center of Kyoto University.

#### A. Double $K$ -Hole Production Probability

The double  $K$ -hole production probability per  $K$  capture was calculated using Eq. (17) with the numerical value of  $\xi$  evaluated by the method described in the preceding chapter. The probabilities  $P(2)$  found in the present numerical calculations are listed in Table II. For comparison, theoretical values from the PP theory are also given.

The experimental studies on double  $K$ -hole production accompanying  $K$  capture have been summarized and discussed by Stephas.<sup>9</sup> These experiments may be divided into three categories: (a)  $K$ -x-ray- $K$ -x-ray coincidence, (b)  $K$ -x-ray energy shift, and (c)  $4\pi$  detection of the ejected electrons. It is noted that some experimental results include contributions from  $L$ -shell electrons, i.e., internal excitation or ionization of the  $K$  electrons accompanying  $L$  capture and that of  $L$  electrons associated with  $K$  capture. The correction for these effects is particularly important for the case of (c)-type experiments. According to the calculations of Wolfsberg,<sup>38</sup> the experimental results of Miskel and Perlman<sup>27</sup> for  ${}^{37}\text{Ar}$  should be reduced by 18% due to the  $L$ -shell contributions.

The experimental values for  ${}^{37}\text{Ar}$  and  ${}^{55}\text{Fe}$  are about twice as high as the theoretical predictions.

The same holds for the earlier experiments on  ${}^{131}\text{Cs}$  and  ${}^{165}\text{Er}$ . However, Nagy, Schupp, and Hurst<sup>35</sup> have recently measured double  $K$ -hole production probabilities for these nuclides by detection of the coincident  $K$  x rays using one NaI(Tl) and one Si(Li) detector. Their experimental values are smaller than the previous results by a factor of 2, and are in better agreement with the present calculated data than the prediction of the PP theory. Nagy, Schupp, and Hurst<sup>35</sup> pointed out that the larger values in the past could have come from various contaminant peaks included in the x-ray peak observed with detectors of poorer resolution.

#### B. Total Ionization Probability

Using the relativistic matrix element with relativistic screening constant, the total  $K$ -shell internal ionization probability per  $K$  capture,  $P_{ej}$ , was calculated from Eq. (14). The integral in this equation was evaluated by Simpson's rule with step size  $h$ . The step size was so chosen that the value of the integral calculated with step size  $h$  agreed with that with step size  $\frac{1}{2}h$  to four significant figures. The total probability calculated in the present work is compared with experimental and previous theoretical results in Table III. For comparison, the values of  $P_{ej}$  calculated from the relativistic theory of Intemann<sup>7,8</sup> taken from Ref. 35, and by the PP theory, are also given in Table III. The present theory yields slightly smaller values than the Intemann theory.

It is noted that, except for the case of  ${}^7\text{Be}$ , the total ionization probabilities from the present

TABLE II. Comparison of theoretical probabilities per  $K$  capture of the double  $K$ -hole production with measured ones.

Nuclide	$\xi$	Theoretical, $10^5 P(2)$		Experimental, $10^5 P(2)$	Method <sup>b</sup>	Ref.
		Present theory	PP <sup>a</sup>			
${}^7\text{Be}$	0.862	$2.63 \times 10^3$ <sup>c</sup>	$7.68 \times 10^2$ <sup>c</sup>			
${}^{37}\text{Ar}$	0.715	23.0	38.6	$44 \pm 8$	C	27, 28
${}^{55}\text{Fe}$	0.697	15.8	18.5	$37 \pm 9$	C	29
${}^{71}\text{Ge}$	0.697	8.85	12.2	$38 \pm 17$	A	30
${}^{131}\text{Cs}$	0.687	1.79	4.13	$13.3 \pm 1.4$	C	31
				$13 \pm 8$	B	32
				$5.0 \pm 1.0$	A	33
${}^{165}\text{Er}$	0.715	1.09	2.70	$2.5 \pm 0.2$	A	28
				$2.0 \pm 1.3$	A	34
				$1.33 \pm 0.33$	A	35
				$1.5 \pm 0.4$	A	36
				$0.67 \pm 0.39$	A	35

<sup>a</sup> PP refers to the theory of Primakoff and Porter.  $\xi = \frac{2}{3}$  has been used.

<sup>b</sup> A, B, and C denote  $K$ -x-ray- $K$ -x-ray coincidence experiment,  $K$ -x-ray energy shift measurement, and  $4\pi$  detection of ejected electrons, respectively.

<sup>c</sup> There are two branches of electron-capture decay, but these values are equal for each of the branches.

TABLE III. Comparison of calculated probabilities per  $K$  capture of the  $K$ -electron ejection with measured ones.

Nuclide	Theoretical, $10^5 P_{ej}$			Experimental, $10^5 P_{ej}$			Ref.	
	Present theory	PP <sup>a</sup>	$I^b$	Experiment	Stephas <sup>c</sup>	Present work <sup>d</sup>		
<sup>7</sup> Be	$1.69 \times 10^3$ <sup>e</sup>	$0.929 \times 10^3$ <sup>e</sup>						
<sup>37</sup> Ar	14.2	27.7						
<sup>55</sup> Fe	8.81	11.2			$36 \pm 17$	$21 \pm 10$	30	
<sup>71</sup> Ge	4.56	6.68		$7.8 \pm 0.7$			31	
<sup>131</sup> Cs	0.709	1.62	0.982		$11 \pm 5$	$6.7 \pm 2.6$	32	
					$4.8 \pm 1.0$	$2.0 \pm 0.4$	33	
					$2.3 \pm 0.2$	$0.99 \pm 0.08$	28	
					$1.8 \pm 1.3$	$0.79 \pm 0.51$	34	
					$1.26 \pm 0.33$	$0.53 \pm 0.13$	35	
<sup>165</sup> Er	$3.23 \times 10^{-2}$ <sup>f</sup>	$4.41 \times 10^{-2}$ <sup>f</sup>	$8.3 \times 10^{-2}$ <sup>f, g</sup>	$(8.4 \pm 1.5) \times 10^{-2}$ <sup>f</sup>			39	
						$1.4 \pm 0.4$	$0.42 \pm 0.11$	36
						$0.62 \pm 0.36$	$0.19 \pm 0.11$	35

<sup>a</sup> Nonrelativistic theory of Primakoff and Porter.

<sup>b</sup> Intemann's relativistic theory, quoted from Ref. 35.

<sup>c</sup> Estimated from  $P(2)$  by Stephas using Schwartz's results (Ref. 9).

<sup>d</sup> Estimated from  $P(2)$  using the present work.

<sup>e</sup> There are two branches of electron-capture decay, but these values are equal for each of the branches.

<sup>f</sup> Energy range 80–354 keV.

<sup>g</sup> Quoted from Ref. 39.

work are lower than the prediction of the PP theory, in contrast to the previous conclusion that relativistic effects would increase the total ionization probability.<sup>28</sup> This conclusion, however, was drawn from a statement of Levinger,<sup>15</sup> who surmised that for the  $K$  electrons of Pb the total internal ionization probability accompanying  $\beta^-$  decay might increase by taking account of relativistic effects. Intemann<sup>8</sup> claimed that extrapolation of Levinger's results to the electron-capture case is incorrect since relativistic effects were estimated using relativistic Coulomb wave functions with nonrelativistic screening constants.

To demonstrate the relativistic effects and the effect of the screening constant on the internal ionization process, the values of the square of the atomic matrix element for <sup>55</sup>Fe, multiplied by  $(1/2\pi^2)\rho W$ , are plotted in Fig. 1 for three different cases:

(1) relativistic theory with relativistic screening constant, (2) relativistic theory with  $\sigma = 0.5$ , and (3) the PP theory. As has been pointed out by Stephas,<sup>9</sup> the relativistic matrix elements with the nonrelativistic screening constant have larger values than the nonrelativistic ones for all energies. However, a curve obtained from the relativistic matrix elements with relativistic screening constant is below the PP curve in the low-energy region and above it in the high-energy region.

It is clear from the figure that relativistic effects increase the internal ionization probability when the nonrelativistic screening constant is used in the relativistic theory. This is the case of the

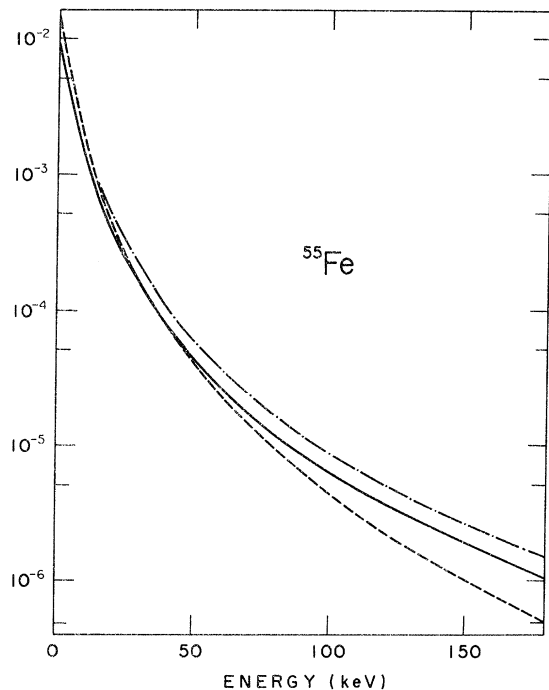


FIG. 1. Square of atomic matrix element, multiplied by  $(1/2\pi^2)\rho W$ , for  $K$ -electron ejection accompanying  $K$ -capture decay of <sup>55</sup>Fe. The solid curve has been calculated from relativistic wave functions with relativistic screening constants; the dot-dashed curve from relativistic wave functions with nonrelativistic screening constants; the dashed curve is from a nonrelativistic calculation.

internal ionization accompanying  $\beta^-$  decay where the screening constant is supposed to be zero since its inclusion has little influence on the probability.

On the other hand, the choice of the screening constant is of critical importance in the internal ionization process during electron capture. It is evident from Fig. 1 and Table III that the relativistic calculations with the relativistic screening constant do reduce the total probability. This conclusion is in agreement with that of Intemann.<sup>8</sup>

Langevin<sup>31</sup> has measured the total ionization probability for  $^{71}\text{Ge}$  by subtracting the main  $K$  Auger and the Auger sum peaks from the observed electron spectrum, and claimed good agreement with the prediction of the PP theory. His result, however, would include the contributions from  $L$ -shell electrons as described in the preceding section.

Since there has been only one experimental value of  $P_{ej}$  reported by Langevin,<sup>31</sup> Stephas<sup>9</sup> compared his theoretical values of  $P_{ej}$  with the numerical values estimated from the experimental values of  $P(2)$  where he used the theoretical results of Schwartz<sup>40</sup> giving the matrix element  $M_{Kn}$  in the form of an inverse- $Z^2$  expansion using nonrelativistic hydro-

genic wave functions. The values thus obtained indicate that the contribution from the internal excitation process is expected to be small. On the contrary, comparison of the present values of  $P_{ej}$  with those of  $P(2)$  in Table II indicates that the internal excitation process has a large contribution to  $P(2)$ . This conclusion agrees well with the Langevin experiment and also with the PP theory. Taking account of this fact, the experimental values of  $P_{ej}$  to be compared with other theoretical calculations were estimated from the experimental values of  $P(2)$  by multiplying the theoretical ratio  $P_{ej}/P(2)$  from the present work. In Table III, the experimental values of  $P_{ej}$  estimated by Stephas and those obtained by us are listed. The values estimated by Stephas are considerably higher than the values predicted by all three theories. However, because of large experimental errors, some experimental data seem to be in agreement with the PP and Intemann theories within experimental errors. On the other hand, the experimental values estimated by us are in better agreement with the theoretical predictions than Stephas values.

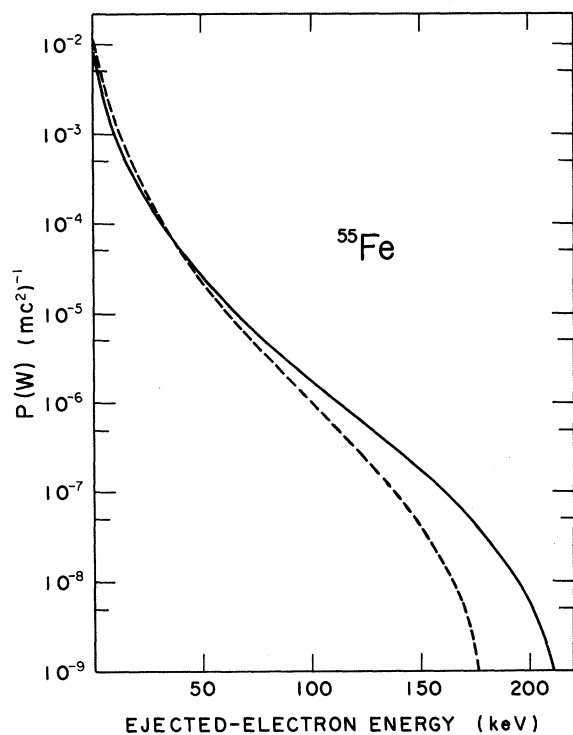


FIG. 2. Energy spectrum of electrons ejected from the  $K$  shell accompanying  $K$ -capture decay of  $^{55}\text{Fe}$ . The solid curve represents the relativistic prediction of the present theory, while the dashed curve represents the Primakoff-Porter theory.

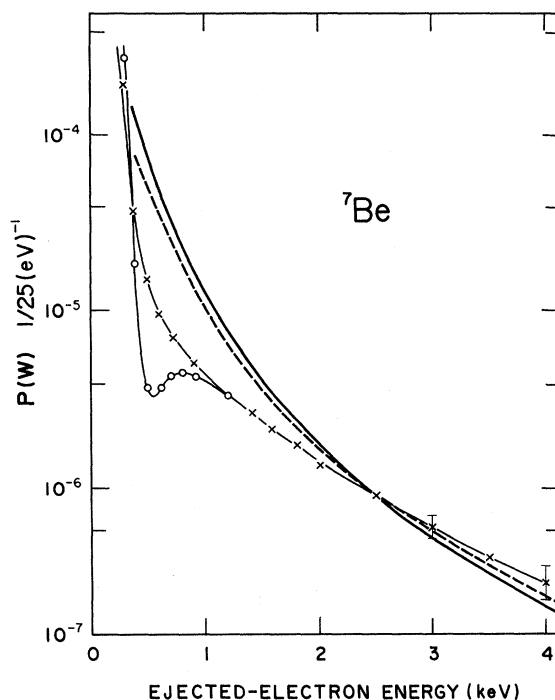


FIG. 3. Spectral distribution of the ejected electrons during  $K$ -capture decay of  $^7\text{Be}$ . The experimental data are denoted by  $\times$  and those corrected for resolution are given by  $\circ$  (Ref. 41). The theoretical spectra have been calculated using the present theory (solid curve) and using the Intemann theory (dashed curve, from Ref. 41). The experimental values have been normalized at 2.5 keV to the present theory and the Intemann's curve has been multiplied by a factor of 1.50.



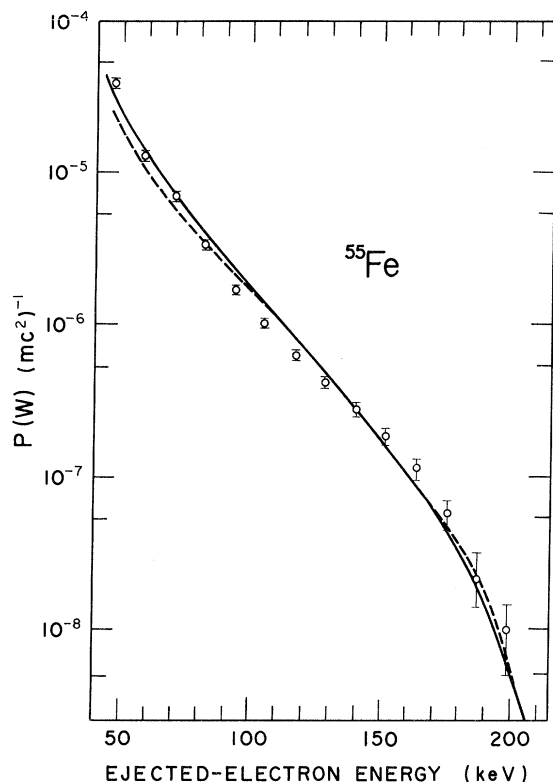


FIG. 4. Spectral distribution of the ejected electrons during  $K$ -capture decay of  $^{55}\text{Fe}$  (Ref. 43). The theoretical spectra have been calculated using the present theory (solid curve) and using the Intemann theory (dashed curve, from Ref. 43). The experimental data have been normalized at 140 keV to the present theory and the Intemann's curve has been multiplied by a factor of 0.764.

Sujkowski *et al.*<sup>39</sup> have recently reported a measurement on the electron-capture decay of  $^{131}\text{Cs}$ . Using a Si(Li) detector placed at the focusing point of a homogeneous-magnetic-field spectrometer to eliminate the interference of electromagnetic radiation, they observed the electron spectrum and obtained the internal ionization probability for the ejected electrons with kinetic energy greater than 80 keV. Their result agrees well with the theoretical value calculated according to the Intemann theory, but is higher by a factor of 2 than that obtained from the present theory.

### C. Spectral Shape of Ejected Electrons

The spectral distribution of the ejected electrons can be calculated using Eq. (13). The ejected-electron spectrum during  $K$  capture of  $^{55}\text{Fe}$  is shown in Fig. 2. For comparison, the nonrelativistic spectrum predicted by the PP theory is also plotted. It can be seen from the figure that

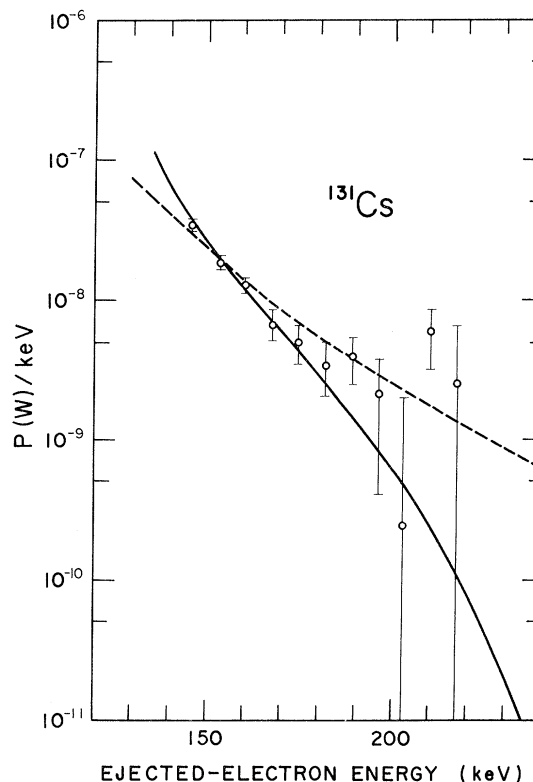


FIG. 5. Spectral distribution of the ejected electrons during  $K$ -capture decay of  $^{131}\text{Cs}$  (Ref. 39). The solid curve represents the present theory, while the dashed curve represents the Intemann theory (Ref. 39).

the prediction of the present calculations is slightly smaller than that of the PP theory in the low-energy region but larger in the high-energy region; the crossover point is near 40 keV. This result is in good agreement with the Intemann theory.<sup>8</sup> The theoretical spectra calculated from the present theory are compared with the experiments in Figs. 3–5.

Mutterer<sup>41</sup> has observed the ejected-electron spectrum in the decay of  $^7\text{Be}$  using a proportional counter. He also measured a spectrum in coincidence with  $\gamma$  rays to see the difference between the ejected-electron spectra for the two electron-capture branches of this nuclide. Nevertheless, both spectra have approximately the same shape and it is impossible to compare them quantitatively because of the  $\gamma$ -ray effect. In Fig. 3, the experimental spectrum is compared with the theoretical spectra calculated by the present theory and the theory of Intemann. Since the ejected-electron spectra calculated for the two branches differ too slightly to be distinguished in the figure, the spectrum for the branch to the ground state of  $^7\text{Li}$  is plotted in the figure. The experi-

mental spectrum is normalized at 2.5 keV to the value of the present theory and the Intemann curve is multiplied by a factor of 1.50 to fit the experimental data.

Measurements of the ejected-electron spectrum for  $^{55}\text{Fe}$  have been performed by Pengra and Crasemann.<sup>42</sup> They employed a proportional counter as an electron detector in the energy range from 25 to 80 keV, while for higher energies an  $n$ - $p$  junction detector was used. The electron spectrum was observed in coincidence with Mn  $K$  x rays detected with the NaI(Tl) detector. However, Stephas<sup>9</sup> suggested from his linearized plot of the experimental data the possibility of undetected systematic errors in the proportional-counter measurements.

Recently, Nagy<sup>43</sup> has reported the continuous electron spectrum ejected in the decay of  $^{55}\text{Fe}$ . Using a coincidence-summing spectrometer consisting of two plastic scintillators, he observed the ejected electrons in the energy range from 40 to 170 keV in  $4\pi$  geometry. The energy distribution of ejected electrons thus obtained is shown in Fig. 4. The solid curve is the prediction of the present theory and the dashed curve represents that of the Intemann theory. The experimental data have been normalized to the present theoretical value at 140 keV and the Intemann curve has been multiplied by a factor of 0.764 to compare with the experiment. The shape of both theoretical spectra is similar in the whole energy region, but the present theory is in better agreement with the experiment than the Intemann theory, especially in the low-energy region. It is noted that in the whole energy region the present theory yields lower probability than the Intemann theory.

The energy spectrum of ejected electrons in the energy range between 80 keV and the end point during the decay of  $^{131}\text{Cs}$  has been observed by Sujkow-

ski *et al.*<sup>39</sup> using a Si(Li) detector placed at the focus of a homogeneous-magnetic-field spectrometer. Figure 5 shows the experimental shape of the energy distribution estimated from the transmission of the magnetic spectrometer, the response function of the semiconductor detector, and the absolute activity of the source. The solid curve represents the relativistic theory of the present work and the dashed curve shows the Intemann theory.

## VI. CONCLUSIONS

Theoretical calculations have been performed of the double  $K$ -hole production probability and the internal ionization probability accompanying  $K$ -electron capture, using relativistic hydrogenic wave functions and relativistic screening constants.

Comparison of experimental values with the theoretical predictions is not conclusive because of the limited amount of experimental data and lack of mutual agreement. Moreover, the large experimental errors make it difficult to discuss the relative merits of the present theory and the previous theories. It is, however, concluded that relativistic effects do reduce the total internal ionization probability, and that the theoretical values calculated according to the present theory are in agreement with the more recent experimental data.

The shape of the energy spectrum of the ejected electrons estimated from the present calculations is similar to that obtained from previous theories, and agrees well with the experimental results.

More elaborate experimental work is needed with high-energy-resolution x-ray detectors. Theoretical and experimental studies on the contributions of  $L$ -shell electrons would also be of great importance. In this respect, it should be useful to perform a triple-coincidence experiment between two  $K$  x rays and the ejected electron.

<sup>1</sup>E. L. Feinberg, J. Phys. USSR 4, 423 (1941).

<sup>2</sup>A. Migdal, J. Phys. USSR 4, 449 (1941).

<sup>3</sup>S. Shimizu, U. S. Atomic Energy Commission Report No. CONF-720404 (unpublished), Vol. 3, p. 2050, and references therein.

<sup>4</sup>P. Benoist-Gueutal, C. R. Acad. Sci. B 230, 624 (1950).

<sup>5</sup>H. Primakoff and F. T. Porter, Phys. Rev. 89, 930 (1953).

<sup>6</sup>R. L. Intemann and F. Pollock, Phys. Rev. 157, 41 (1967).

<sup>7</sup>R. L. Intemann, Phys. Rev. 178, 1543 (1969).

<sup>8</sup>R. L. Intemann, Phys. Rev. 188, 1963 (1969).

<sup>9</sup>P. Stephas, Phys. Rev. 186, 1013 (1969).

<sup>10</sup>P. Stephas and B. Crasemann, Phys. Rev. 164, 1509 (1967).

<sup>11</sup>P. Stephas and B. Crasemann, Phys. Rev. C 3, 2495 (1971).

<sup>12</sup>T. Kitahara, Y. Isozumi, and S. Shimizu, Phys. Rev. C 5, 1810 (1972).

<sup>13</sup>J. N. Bahcall, Phys. Rev. 129, 2683 (1963).

<sup>14</sup>E. J. Konopinski, *The Theory of Beta Radioactivity* (Oxford U. P., London, 1966), p. 234.

<sup>15</sup>J. S. Levinger, Phys. Rev. 90, 11 (1953).

<sup>16</sup>M. E. Rose, *Relativistic Electron Theory* (Wiley, New York, 1961), p. 179.

<sup>17</sup>Reference 16, p. 194.

<sup>18</sup>J. C. Jaeger and H. R. Hulme, Proc. R. Soc. A148, 708 (1935).

<sup>19</sup>Reference 16, p. 177.

<sup>20</sup>D. R. Hartree, *The Calculation of Atomic Structures* (Wiley, New York, 1957).

<sup>21</sup>J. L. Campbell, L. A. McNelles, and J. Law, Can. J. Phys. 49, 3142 (1971).

<sup>22</sup>T. A. Carlson, C. W. Nestor, Jr., T. C. Tucker, and

- F. B. Malik, Phys. Rev. 169, 27 (1968).
- <sup>23</sup>W. Magnus, F. Oberhettinger, and R. P. Soni, *Formulas and Theorems for the Special Functions of Mathematical Physics* (Springer-Verlag, Berlin, 1966), p. 64.
- <sup>24</sup>T. A. Carlson, C. C. Lu, T. C. Tucker, C. W. Nestor, and F. B. Malik, Oak Ridge National Laboratory Report No. ORNL-4614, 1970 (unpublished).
- <sup>25</sup>J. C. Slater, Phys. Rev. 36, 57 (1930).
- <sup>26</sup>F. Herman and S. Skillman, *Atomic Structure Calculations* (Prentice-Hall, Englewood Cliffs, N. J., 1963).
- <sup>27</sup>J. A. Miskel and M. L. Perlman, Phys. Rev. 94, 1683 (1954).
- <sup>28</sup>N. L. Lark and M. L. Perlman, Phys. Rev. 120, 536 (1960).
- <sup>29</sup>R. W. Kiser and W. H. Johnston, J. Am. Chem. Soc. 81, 1810 (1959).
- <sup>30</sup>G. Charpak, C. R. Acad. Sci. B 237, 243 (1953).
- <sup>31</sup>M. Langevin, C. R. Acad. Sci. B 245, 664 (1957); J. Phys. Radium 19, 34 (1958).
- <sup>32</sup>W. von Oertzen, Z. Phys. 182, 130 (1964).
- <sup>33</sup>H. Daniel, G. Schupp, and E. N. Jensen, Phys. Rev. 117, 823 (1960).
- <sup>34</sup>K. M. Smith, University of Glasgow (unpublished), quoted from Ref. 9.
- <sup>35</sup>H. J. Nagy, G. Schupp, and R. R. Hurst, Phys. Rev. C 6, 607 (1972).
- <sup>36</sup>H. Ryde, L. Persson, and K. Oelsner-Ryde, Nucl. Phys. 47, 614 (1963).
- <sup>37</sup>C. M. Lederer, J. M. Hollander, and I. Perlman, *Table of Isotopes* (Wiley, New York, 1967), 6th ed.
- <sup>38</sup>M. Wolfsberg, Phys. Rev. 96, 1712 (1954).
- <sup>39</sup>Z. Sujkowski, B. Myslek, J. Lukasiak, and B. Kotlińska-Filipek, U. S. Atomic Energy Commission Report No. CONF-720404 (unpublished), Vol. 3, p. 2005.
- <sup>40</sup>H. M. Schwartz, J. Chem. Phys. 21, 45 (1953).
- <sup>41</sup>M. Mutterer, U. S. Atomic Energy Commission Report No. CONF-701002 (unpublished), p. 452.
- <sup>42</sup>J. G. Pengra and B. Crasemann, Phys. Rev. 131, 2642 (1963).
- <sup>43</sup>J. Nagy, ATOMKI Köz. 13, 101 (1971).